

# GAMMA-DECAY IN LIGHT NUCLEI. BORROMEAN HALO, TANGO HALO, AND HALO ISOMERS

Izosimov I.N.

*Joint Institute for Nuclear Research, 141980, Dubna, Russia, e-mail: izosimov@jinr.ru*

## INTRODUCTION

Generally the term halo is used when halo nucleon(s) spend(s) at least 50% of the time outside the range of the core potential, i.e. in the classically forbidden region [1–3]. The necessary conditions for the halo formation are: the small binding energy of the valence particle(s), small relative angular momentum  $L=0, 1$  for two-body or hyper momentum  $K=0, 1$  for three-body halo systems, and not so high level density (small mixing with non-halo states). Coulomb barrier may suppresses proton-halo formation for  $Z > 10$ . Neutron and proton halos have been observed in several nuclei [1–3]. In Borromean systems the two-body correlations are too weak to bind any pair of particles while the three-body correlations are responsible for the system binding as a whole. In states with one and only one bound subsystem the bound particles moved in phase and were therefor named tango states [2]. Halo of Borromean type is well known in atomic nuclei [4]. The Isobar Analog State (IAS) of the  ${}^6\text{He}$  ground state (two-neutron halo nucleus), i.e., the 3.56 MeV,  $J=0^+$  state of  ${}^6\text{Li}$ , has [5, 6] a neutron-proton halo structure of Borromean type. In the general case [7] the IAS is the coherent superposition of the excitations like neutron hole–proton particle coupled to form the momentum  $J=0^+$ . The IAS has the isospin  $T=T_Z+1=(N-Z)/2+1$ , where  $T_Z=(N-Z)/2$  is the isospin projection. The isospin of the ground state is  $T=T_Z=(N-Z)/2$ . When the IAS energy corresponds to the continuum, the IAS can be observed as a resonance. Configuration states (CS) are not the coherent superposition of such excitations and have  $T=T_Z=(N-Z)/2$ . One of the best studied CS is the anti-analog state (AIAS) [7, 8]. The CS formation may be restricted by the Pauli principle. The Double Isobar Analog State (DIAS) has the isospin  $T=T_Z+2$  and is formed as the coherent superposition of the excitations like two neutron holes–two proton particles coupled to form the momentum  $J=0^+$ . For the IAS, CS, DIAS, and double configuration states (DCS) the proton particles have the same spin and spatial characteristics as the corresponding neutron holes. When the parent state is a two-neutron halo nucleus, IASs and CSs will have the proton-neutron halo structure, DIASs and the DCSs will have the proton-proton halo structure. For nuclei with enough neutrons excess IASs and CSs can have not only the  $p$ - $n$  halo component but also the  $n$ - $n$  halo component, DIASs and DCSs can have both  $p$ - $p$ ,  $n$ - $n$ , and  $p$ - $n$  components [8]. IASs, CSs, DIASs, and DCSs can be observed as resonances in nuclear reactions.

Excited halo states and resonances of non-IAS structure may also occur in atomic nuclei [2, 3, 9–12] both from proton-rich and neutron-rich sides. Halo of tango type is well known in molecules [2].

Characteristics of the  $\gamma$ -transitions in  ${}^6\text{Li}$  are analyzed. It is shown that the ground state of atomic nucleus  ${}^6\text{Li}$  ( $J=1^+$ ,  $S_n=5.66$  MeV,  $S_p=4.59$  MeV,  $S_d=1.47$  MeV) may be a good candidate for halo state of tango type.

Strong mixing with other more complicated states dilutes the component of the halo. High level density of non-halo levels prevents halo formation [2] in the excited states. In other words, the distance between non-halo states must be larger than the coupling to the halo state (or non-halo level density is not high). There may be only a small window open for halo occurrence. How small this window is, it can be answered by study halo in excited states.

Isospin symmetry essentially reduced mixing of the configurations with different isospin quantum number and favorable for halo formation. Such excited states and resonances as IAS, DIAS, CS, and DCS in nuclei may simultaneously have  $n$ - $n$ ,  $n$ - $p$ , and  $p$ - $p$  halo components in their wave functions [8]. Differences in halo structure of the excited states (or between excited and ground states) can result [9, 10] in the formation of isomers (halo-isomers). From this point of view some CS and DCS depending on their halo structure, may be observed as halo isomers. Because the small angular momentum is the necessary condition for halo formation, the nuclear reactions with protons and neutrons are attractive for halo isomers excitation.

Structure of the ground and excited states in halo like nuclei is discussed. Values of reduced probability  $B(M\lambda)$  and  $B(E\lambda)$  for  $\gamma$ -transitions in  ${}^{6,7,8}\text{Li}$ ,  ${}^{8,9,10}\text{Be}$ ,  ${}^{8,10,11}\text{B}$ ,  ${}^{10,11,12,13,14}\text{C}$ ,  ${}^{13,14,15,16,17}\text{N}$ ,  ${}^{15,16,17,19}\text{O}$ , and  ${}^{17}\text{F}$  are analyzed. Special attention is given to nuclei whose ground state does not exhibit halo structure but the excited state may have one.

### 1. ISOBAR ANALOGUE STATES, DOUBLE ISOBAR ANALOGUE STATES, CONFIGURATION STATES, AND DOUBLE CONFIGURATION STATES

Analogue states (analog) in nuclei are of interest for both theoretical and experimental investigations. There are two main points that are decisive for the isospin  $T$  being a good quantum number in both light and heavy nuclei:

1. Charge independence of nuclear forces acting between nucleons.
2. A number of factors that weaken violation of the charge independence of forces in a nucleus by Coulomb forces [7].

As a result, in a nucleus there can be (Fig.1) several systems of levels (resonances) that differ in isospin  $T$  ( $T_0, T_0+1, \dots$ ),  $T_0 = (N - Z)/2$ . If  $T = T_{Z^+} + 1$ , these are so-called analogue states; if  $T = T_{Z^+} + 2$ , these are double analogue states, and so on. Analogue states that fall within the continuum region are also referred to as analogue resonances.

Analogue states for  $N > Z$  ( $T_Z > 0$ ) nuclei are formed from the initial state ( $T, T = T_Z$ ) through various replacements of a neutron by a proton in the same state. The wave function of the analog involves excitations like proton particle–neutron hole coupled to form the momentum  $J = 0^+$  which are not forbidden by the Pauli principle. Levels with the identical  $T$  are in the neighboring nuclei and are shifted relative to each other by  $\Delta E_c - \delta$ , where  $\Delta E_c$  is the Coulomb energy of the added proton and  $\delta$  is the mass difference of the neutron and the proton. The analog structure for  $N > Z$  nuclei can be obtained by applying the operator:

$$T_- = \sum a_i^+(p) \cdot a_i^-(n), \quad (1)$$

and the double analog structure is obtained by twice applying the nucleus isospin ladder operator  $T_-$  to the ground state of the parent nucleus.  $T_-$  is the operator for transformation of the neutron to the proton without a change in the function of the state in which the particle is; i.e., in (1)  $a_i^-(n)$  is the operator for annihilation of the neutron in the state  $i$ , and  $a_p^i(p)$  is the operator for production of the proton in the state  $i$ . By virtue of the Pauli principle, the summation is limited to the states which are filled with the excess neutrons.

The wave function of the analog state is written as:

$$\psi_{T_0+1, T_0}^{IAS} = \frac{1}{\sqrt{2(T+1)}} T_- \psi_{T_0+1, T_0+1}^{PS}, \quad (2)$$

Here  $\psi_{T_0+1, T_0+1}^{PS}$  is the wave function for the parent states with the isospin  $T = T_0 + 1$  and the isospin projection  $T_Z = T_0 + 1$  (Fig.1). The analogue state turns out to be sharply distinguished in many properties because its isospin is greater by one than the isospin of the neighboring states. The experimental and theoretical data indicate that the mixing of states with different isospins is insignificant and the individual character of analogue states distinctly manifests itself in many experiments.

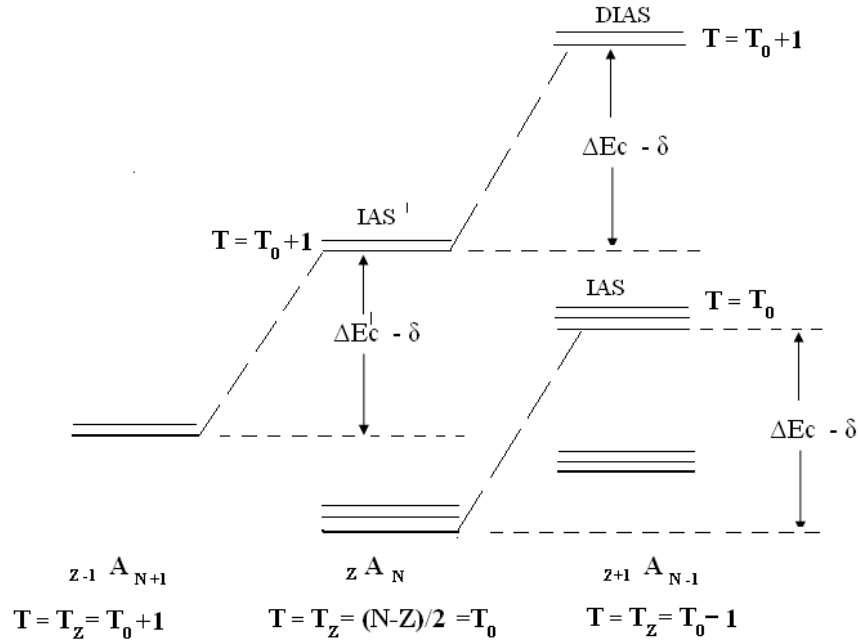


Fig.1. Diagram of analogue (IAS) and double analogue (DIAS) states.

For nuclear ground states the isospin is equal to the isospin projection  $T = T_Z = (N - Z)/2$ . The analogue state differs in isospin by one from the neighboring states, and the isospin of the analogue state is greater by one than the isospin projection  $T = T_Z + 1$ . For the double analogue state  $T = T_Z + 2$ .

The analogue state is a collective state, which is coherent superposition of elementary excitations like proton particle–neutron hole coupled to form the momentum  $J = 0^+$ , i.e., all elementary excitations enter into the wave function of the analog with one sign (Fig.2). Accordingly, the double analogue state is coherent superposition of elementary excitations like two protons–two neutron holes coupled to form the momentum  $J = 0^+$ .

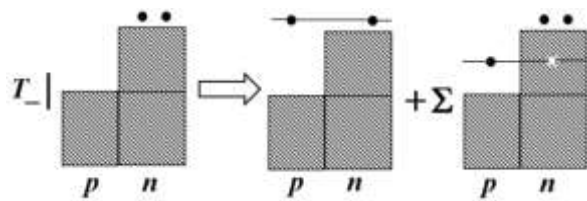


Fig. 2. Structure of the IAS wave function when the parent state has the  $n$ - $n$  halo. The IAS wave function involves two components corresponding to the  $p$ - $n$  and  $n$ - $n$  halo.

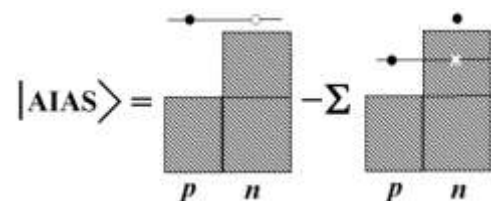


Fig. 3. Structure of the AIAS wave function when the parent state has the  $n$  halo. The anti-analog wave function involves two components corresponding to the  $p$  and  $n$  halo.

If the elementary excitations enter into the wave function incoherently, so-called configuration states are formed. In halo like nuclei formation of configuration states can be associated with core excitation, and in some case it can be forbidden by the Pauli principle. The isospin of the configuration states is smaller the analog isospin by one, and the excitation energy of the configuration states is also lower than the analog excitation energy. One of the best studied configuration states is (Fig.3) the anti-analog [7, 13] state (AIAS). Since transformation of the neutron to the proton during the formation of analog, double analog, configuration states, and double configuration states is not followed by a change in the spatial and spin characteristics, the above excited states in the halo like nuclei will also have a halo like structure. Let us take as the parent state the wave function for the ground state of the nucleus in which two neutrons make up the nuclear halo ( $n$ - $n$  halo) and act on it by the operator  $T_-$  (Fig.2). As a result, we find that the wave function for the analogue state and configuration states involves components corresponding to the proton-neutron halo ( $n$ - $p$  halo) and two-neutron halo ( $n$ - $n$  halo). For some nuclei configuration states are not formed by virtue of the Pauli principle, and the analog wave function can lack the component corresponding to the  $n$ - $n$  halo. Let us act by the operator  $T_-$  on the ground state wave function for the  $n$ - $n$  halo nucleus once more (Fig.4).

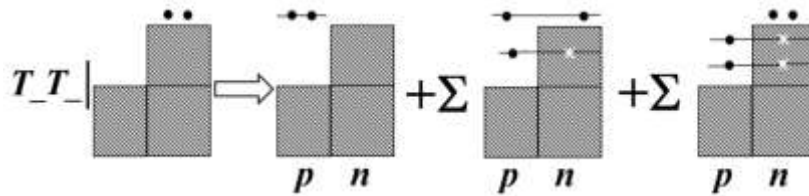


Fig. 4. Structure of the DIAS wave function when the parent state has the  $n$ - $n$  halo. The DIAS wave function involves three components corresponding to the  $p$ - $p$ ,  $p$ - $n$ , and  $n$ - $n$  halo.

We find that the wave function for the double analogue state and double configuration states has the components corresponding to the  $p$ - $p$ ,  $p$ - $n$ , and  $n$ - $n$  halo. For some nuclei there can be no  $p$ - $n$  and  $n$ - $n$  halo components by virtue of the Pauli principle.

When  $T_Z < 0$  the all previous reasonings and conclusions concerning nuclei with  $Z > N$  remain in force under the substitution of  $T_-$  for  $T_+$ :

$$T_+ = \sum a_i^+ (n) \cdot a_i^- (p), \quad (3)$$

The corresponding configurations for nuclei with  $Z > N$  are now formed under substitution of proton with neutron, which has similar spin and spatial state characteristics. Thus in  $Z > N$  nuclei, proton-particle and neutron-hole elementary excitations coupled to form the momentum  $J= 0^+$  are replaced by elementary excitations, like neutron-particle and proton-hole coupled to form the momentum  $J= 0^+$ . Thus the following conclusion can be drawn [8]:

A) Such excited states and resonances as isobar analog, double isobar analog, configuration states, and double configuration states in halo nuclei can also have a halo like structure of different types ( $n$ - $n$ ,  $p$ - $p$ ,  $p$ - $n$ ).

B) Isobar analog, double isobar analog, configuration states, and double configuration states can simultaneously have  $n$ - $n$ ,  $n$ - $p$ , and  $p$ - $p$  halo components in their wave functions.

C) Structure of the halo may be different for the different levels and resonances in atomic nuclei.

## 2. CLASSIFICATION AND SYSTEMATIC OF THE $\gamma$ - TRANSITIONS USING ISOSPIN

Isvector (IV) and isoscalar (IS) parts [7] may be separated in the  $\gamma$ -transition operator. For IV/IS  $\gamma$ -transition only IV/IS part of  $\gamma$ -transition operator gives contribution to the probability of  $\gamma$ -decay. Selection rules on isospin for  $\gamma$ -transitions are:  $\Delta T = 0, \pm 1$ ;  $\Delta T_Z = 0$ . For  $\Delta T = \pm 1$  only isovector part of operator gives contribution to the matrix element (IV-transitions). For  $\Delta T = 0$  ( $T \neq 0$ ) – both isovector and isoscalar parts of operator give contribution (mixture of IV and IS). For  $N=Z$  ( $T_Z=0$ ) isovector component does not give contribution to the transitions between  $T=0$  states (IS-transitions). For E1  $\gamma$ -decay only isovector part gives contribution to the matrix element and E1  $\gamma$ -transitions between  $T=0$  states are forbidden on isospin in  $N=Z$  nuclei. Recommended [14–17] upper limits for  $B(E,\lambda)$  and  $B(M,\lambda)$  are presented in the Table1. Systematics of IV/IS  $\gamma$ -transitions are given in [7].

Table 1. Upper limits[12–15] for the  $\Gamma_\gamma/\Gamma_w=B(E,\lambda)/B(E,\lambda)_w$  or  $B(M,\lambda)/B(M,\lambda)_w$ ,

transition	$\Gamma_\gamma/\Gamma_w$ upper limit		
	$A=6-44^a$	$A=45-150$	$A>150$
E1 (IV)	0.3 <sup>b</sup>	0.01	0.01
E2 (IS) <sup>c</sup>	100	300	1000
E3	100	100	100
E4	100	100 <sup>d</sup>	
M1 (IV)	10	3	2
M2 (IV)	3	1	1
M3 (IV)	10	10	10
M4		30	10

$\Gamma_\gamma$  –  $\gamma$ -width, ‘w’ – Weisskopf estimates. <sup>a</sup>  $\Gamma_\gamma/\Gamma_w$  (upper limit)=10 – for E2 (IV); 0.03 – for M1 (IS); 0,1 – for M2 (IS); 0,003 – for E1 ( $T=0$  states, due to isospin mixture). <sup>b</sup>  $\Gamma_\gamma/\Gamma_w$  (upper limit) = 0,1 for  $A=21-44$ . <sup>c</sup> In super deformed bands  $\Gamma_\gamma/\Gamma_w>1000$  for E2 transitions may be observed. <sup>d</sup>  $\Gamma_\gamma/\Gamma_w$  (upper limit) = 30 for  $A=90-150$ .

In the  $20 \leq A \leq 40$  nuclei contribution of the isoscalar part for  $\gamma$ -transitions is about: for M1  $\gamma$ -transitions – 0.01; for M2  $\gamma$ -transitions – 0.01; for ML,  $L>2$   $\gamma$ -transitions – 0.2; for E1  $\gamma$ -transitions about 0.03 ( $T$ -forbidden transitions, isospin mixture about 3%).

Table 2. Systematic of the  $\gamma$ -transitions in the  $5 \leq A \leq 40$  nuclei [7]. W.u. – Weisskopf unit.

<u>E1 <math>\gamma</math>-transitions.</u>
A) T-allowed ( $\Delta T = 1, T_Z=0$ ; $\Delta T = 0, \pm 1, T_Z \neq 0$ ). $\langle B(E1) \rangle \approx 0.0026$ W.u.
B) T-forbidden ( $\Delta T=0, T_Z=0$ ), $\langle B(E1) \rangle \approx 0.0003$ W.u., hindrance factor $\approx 7$ for $N=Z$ .
<u>M1 <math>\gamma</math>-transitions.</u>
A) T-favorable (only IV part of $\gamma$ -transition operator gives contribution, $\Delta T = \pm 1$ ). $\langle B(M1) \rangle \approx 0.38$ W.u.
B) T-usual (both IV and IS parts of $\gamma$ -transition operator give contribution, $\Delta T = 0$ , $T_Z \neq 0$ ). $\langle B(M1) \rangle \approx 0.10$ W.u.
C) T-hindered (only IS part of $\gamma$ -transition operator gives contribution, $\Delta T=0$ ; $T_Z=0$ ). $\langle B(M1) \rangle \approx 0.0048$ W.u.
<u>M2 <math>\gamma</math>-transitions.</u>
A) T-favorable. $\langle B(M2) \rangle \approx 0.31$ W.u.
B) T-hindered. $\langle B(M2) \rangle \approx 0.1$ W.u.

For EL  $\gamma$ -transitions with  $L \geq 2$  it is difficult to make some conclusion about contribution of the isoscalar part. On isospin quantum number the  $\gamma$ -transitions may be classify [7] as (Table 2) favorable ( $\Delta T = 1; T_Z = 0$ ), usual ( $\Delta T = 0, \pm 1; T_Z \neq 0$ ), hindered ( $\Delta T = 0; T_Z = 0$ ).

### 3. ${}^6\text{He}$ NUCLEUS (BORROMIAN $n$ - $n$ HALO) AND ${}^6\text{Li}$ NUCLEUS (BORROMIAN $n$ - $p$ HALO FOR IAS, TANGO $n$ - $p$ HALO FOR G.S.)

Two neutrons that form the  $n$ - $n$  halo in  ${}^6\text{He}$  ground state occupy the  $1p$  orbit ( $p_{3/2}$  configuration with a 7% admixture of  $p_{1/2}$  configuration). The remaining two neutrons and two protons occupy the  $1s$  orbit. Therefore, the action of the operator  $T_-$  on the ground state wave function for the  ${}^6\text{He}$  nucleus ( $T = 1, T_Z = 1$ ) results in the formation of the analogue state with the configuration corresponding to the  $p$ - $n$  halo. This IAS is in the  ${}^6\text{Li}$  nucleus ( $T = 1, T_Z = 0$ ) at the excitation energy 3.56 MeV. The width of this state is  $\Gamma = 8.2$  eV, which corresponds to the half-life  $T_{1/2} = 6 \cdot 10^{-17}$  s. The experimental data [5,6] indicate that this state has  $n$ - $p$  halo. Formation of configuration states is prohibited by the Pauli principle.

The  $\gamma$ -decay of IAS would be hindered if the ground state of  ${}^6\text{Li}$  did not have a halo structure. The data on lifetime of IAS in  ${}^6\text{Li}$  are given in [18], but the M1  $\gamma$ -decay branch is not determined. If one assumes that the total lifetime of IAS is determined by M1  $\gamma$ -decay, the reduced transition probability would be  $B(M1) = 8.6$  W.u. Assuming the orbital part of the M1  $\gamma$ -transition operator is neglected [7],  $B(M1, \sigma)$  for M1  $\gamma$ -decay of IAS in  ${}^6\text{Li}$  can be determined from the reduced probability  $ft$  of the  ${}^6\text{He}$   $\beta$ -decay (Fig.5).

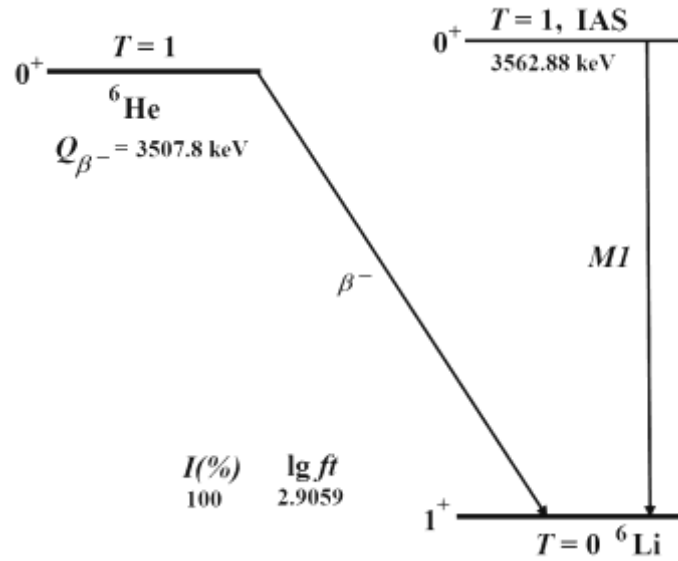


Fig.5. Connection [7] between the  $ft$  value for  $\beta$ -decay of the parent state ( ${}^6\text{He}$  g.s.) and the  $B(M1, \sigma)$  value for  $\gamma$ -decay of the IAS ( ${}^6\text{Li}$ ,  $E=3562$  keV).  $ft = 11633/[T_0 \times B(M1, \sigma)]$ ,  $T_0$ -isospin of the parent state,  $ft$  in sec,  $B(M1, \sigma)$  in  $\mu_0^2$ , for M1  $\gamma$ -transition W.u.= $1.79 \mu_0^2$ ,  $B(M1, \sigma) = 8.2$  W.u.,  $B(M1) \approx 8.6$  W.u.

The  $B(M1, \sigma)$  value proved to be 8.2 W.u., i.e. the probability of the M1  $\gamma$ -transition is close to the value for the upper limit (Table 1) in the light nuclei region. Considerable overlap of wave functions of the two halo states (i.e. the IAS halo state and ground state halo) in  ${}^6\text{Li}$  results in significant increase of the probability of M1  $\gamma$ -transition between the states. In the absence of halo structure in the ground state of  ${}^6\text{Li}$ , a corresponding M1  $\gamma$ -transition would be hindered. A rather large value of the reduced probability of M1  $\gamma$ -transition ( $B(M1, \sigma) = 8.2$  W.u.) for M1  $\gamma$ -decay from IAS to the ground state is evidence for the existence of tango halo structure in the  ${}^6\text{Li}$  ground state. The IAS in  ${}^6\text{Li}$  has the Borromean structure since the  $n$ - $p$

subsystem is coupled to the momentum  $J = 0^+$ , i.e. unbound, whereas  $n-p$  subsystem for the  ${}^6\text{Li}$  ground state is coupled to the momentum  $J = 1^+$ , i.e. bound. According to halo classification [2], such structure of the  ${}^6\text{Li}$  ground state corresponds to the tango halo. Such conclusion agrees with the data on the properties of  ${}^6\text{Li}$  nucleus and on the properties of nuclear reactions with  ${}^6\text{Li}$  beams. The radius of the  ${}^6\text{Li}$  nucleus ranges between 2.32 fm and 2.45 fm, and this is 10% larger than the radius value expected from the available systematics. The  ${}^6\text{Li}$  nucleus is known to have the  $(\alpha + d)$  cluster structure (the energy threshold for the breakup of this nucleus into a deuteron and an alpha particle is as low as 1.47 MeV) [18-20]. The momentum distributions of  ${}^4\text{He}$  from the  ${}^6\text{He}$  and  ${}^6\text{Li}$  breakup were measured for different targets and beam energies. The observed momentum distributions are narrow for the  ${}^6\text{He}$  breakup ( $\sigma = 28-29$  MeV/ $c$ ) and intermediate for the  ${}^6\text{Li}$  breakup ( $\sigma = 46-55$  MeV/ $c$ ) [18-20]. For ordinary (non- halo) nuclei, this value would have been about  $\sigma = 100$  MeV/ $c$ . The small width of the momentum distribution [18-20] confirms the presence of halo in  ${}^6\text{He}$ , and intermediate width of the momentum distribution supports hypothesis of  $n-p$  halo in  ${}^6\text{Li}$ .

#### 4. SYSTEMATIC OF THE $B(M,\lambda)$ AND $B(E,\lambda)$ VALUES FOR $\gamma$ -TRANSITIONS IN ${}^{6,7,8}\text{Li}$ , ${}^{8,9,10}\text{Be}$ , ${}^{8,10,11}\text{B}$ , ${}^{10,11,12,13,14}\text{C}$ , ${}^{13,14,15,16,17}\text{N}$ , ${}^{15,16,17,19}\text{O}$ , AND ${}^{17}\text{F}$ . HALO ISOMERS

Data on  $B(M,\lambda)$  and  $B(E,\lambda)$  from [20-28] were used for analysis of  $\gamma$ -transitions. The parameters for the distributions (Fig.6) of the  $\lg(B(M,\lambda))$  and  $\lg(B(E,\lambda))$  and systematic of the mean values  $\langle B(M,\lambda) \rangle$  and  $\langle B(E,\lambda) \rangle$  for  $\gamma$ -transitions in  ${}^{6,7,8}\text{Li}$ ,  ${}^{8,9,10}\text{Be}$ ,  ${}^{8,10,11}\text{B}$ ,  ${}^{10,11,12,13,14}\text{C}$ ,  ${}^{13,14,15,16,17}\text{N}$ ,  ${}^{15,16,17,19}\text{O}$ , and  ${}^{17}\text{F}$  nuclei are presented in the Tables 3-5.

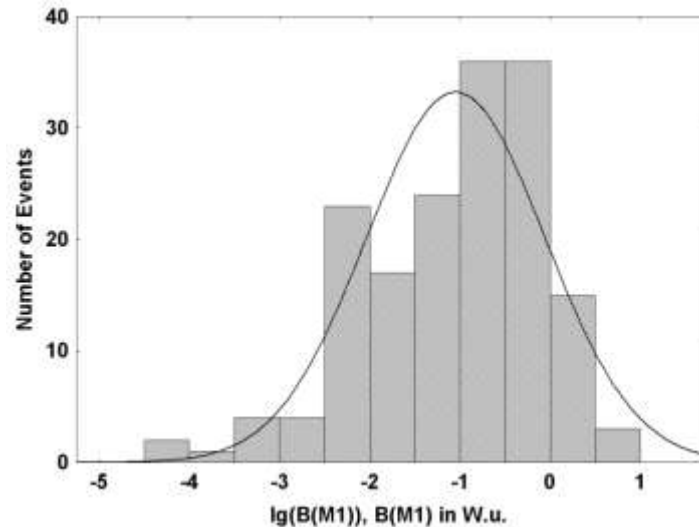


Fig.6. Distribution of the  $\lg(B(M1))$  values for IV, IV+IS, and IS M1  $\gamma$ -transitions in  ${}^{6,7,8}\text{Li}$ ,  ${}^{8,9,10}\text{Be}$ ,  ${}^{8,10,11}\text{B}$ ,  ${}^{10,11,12,13,14}\text{C}$ ,  ${}^{13,14,15,16,17}\text{N}$ ,  ${}^{15,16,17,19}\text{O}$ , and  ${}^{17}\text{F}$ . Mean values:  $\langle \lg(B(M1)) \rangle = -1.0$ ,  $\langle B(M1) \rangle = 0.1$  W.u., standard deviation  $\sigma(\lg(B(M1))) = 0.99$ .

The  $\langle B(M,\lambda) \rangle$  and  $\langle B(E,\lambda) \rangle$  values are in agreement with previous systematics [7,29], but one can indicate the tails for in lower  $\lg(B(M,\lambda))$  and  $\lg(B(E,\lambda))$  value parts of distributions. These tails may be connected with halo isomers and they were the objects of our analysis.

When the halo structure of the excited state differs from that of the ground state, or the ground state has no halo structure, the  $\gamma$ -transition from the excited state to the ground state can be essentially hindered, i.e. the formation of a specific type of isomers (halo isomers) becomes possible. The particularity of halo isomer observations lies in the fact that it is necessary to analyze partial  $\gamma$ -decay lifetime.

The radial factor  $r^\lambda$  for the electric and  $r^{\lambda-1}$  for the magnetic multipole  $\gamma$ -transition operator of order  $\lambda$  may compensate the differences in the large-distance parts of halo and no halo wave functions. Here  $r$  is the core-halo distance. The most sensitive for detection of the  $\gamma$ -transition hindrance between halo–no halo states will be M1  $\gamma$ -transitions (or may be E1 and M2).

Table 3. Parameters of the Gauss distribution for the  $\lg(B(M\lambda))$  values. Gamma-transitions in  ${}^{6,7,8}\text{Li}$ ,  ${}^{8,9,10}\text{Be}$ ,  ${}^{8,10,11}\text{B}$ ,  ${}^{10,11,12,13,14}\text{C}$ ,  ${}^{13,14,15,16,17}\text{N}$ ,  ${}^{15,16,17,19}\text{O}$ , and  ${}^{17}\text{F}$  nuclei.  $B(M\lambda)$  in W.u.  $\langle \lg(B(M\lambda)) \rangle$  – mean value,  $\sigma(\lg(B(M\lambda)))$  – standard deviation for the  $\lg(B(M\lambda))$  distribution. IS/IV – isoscalar/isovector  $\gamma$ -transitions.

Type of the $\gamma$ -transition	All M1 IV, IV+IS, and IS	M1, IV+IS, $\Delta T=0$	M1, IV ( $\Delta T=1$ )	M1, IS, N=Z ( $T=0 \rightarrow T=0$ )	All M2	M2, IV	M2, IV+IS	M2 IS, N=Z
$\langle \lg(B(M\lambda)) \rangle$	-1.0	-1.0	-0.46	-2.07	-0.38	0.09	-0.38	-1.2
$\sigma(\lg(B(M\lambda)))$	0.99	0.87	0.60	1.02	1.0	0.26	0.93	0.9

Table 4. Parameters of the Gauss distribution for the  $\lg(B(E\lambda))$  values. Gamma-transitions in  ${}^{6,7,8}\text{Li}$ ,  ${}^{8,9,10}\text{Be}$ ,  ${}^{8,10,11}\text{B}$ ,  ${}^{10,11,12,13,14}\text{C}$ ,  ${}^{13,14,15,16,17}\text{N}$ ,  ${}^{15,16,17,19}\text{O}$ , and  ${}^{17}\text{F}$  nuclei.  $B(E\lambda)$  in W.u.

Type of the $\gamma$ -transition	All E1	E1, $\Delta T=1$	E1, $\Delta T=0$	E1 ( $T=0 \rightarrow T=0$ , T-forbidden)	All E2	E2, IV ( $\Delta T=1$ )	E2, $\Delta T=0$	E2, IS, N=Z	All E3
$\langle \lg(B(E\lambda)) \rangle$	-2.64	-2.11	-2.54	-3.54	0.15	0.18	0.11	0.22	0.7
$\sigma(\lg(B(E\lambda)))$	1.2	1.1	1.1	1.32	0.87	0.63	0.81	1.0	0.3

Table 5. Systematic of the mean values  $\langle B(M,\lambda) \rangle$  and  $\langle B(E,\lambda) \rangle$  for  $\gamma$ -transitions in  ${}^{6,7,8}\text{Li}$ ,  ${}^{8,9,10}\text{Be}$ ,  ${}^{8,10,11}\text{B}$ ,  ${}^{10,11,12,13,14}\text{C}$ ,  ${}^{13,14,15,16,17}\text{N}$ ,  ${}^{15,16,17,19}\text{O}$ , and  ${}^{17}\text{F}$  nuclei.

<u>E1-transitions</u>
A) T-favorable, $\Delta T = \pm 1$ . $\langle B(E1) \rangle \approx 0.0079$ W.u. B) T-usual, $\Delta T = 0$ ; $T_Z \neq 0$ . $\langle B(E1) \rangle \approx 0.0032$ W.u. C) T-forbidden, $\Delta T=0$ ; $T_Z = 0$ . $\langle B(E1) \rangle \approx 0.00029$ W.u. T-allowed, $\Delta T = 1$ ; $T_Z = 0$ . $\langle B(E1) \rangle \approx 0.006$ W.u. T-forbidden factor $\approx 20$ . D) All, $\Delta T = 0, \pm 1$ ; $\Delta T_Z = 0$ . $\langle B(E1) \rangle \approx 0.0025$ W.u.
<u>E2-transitions</u>
A) $\Delta T = \pm 1$ , $T_Z \neq 0$ . $\langle B(E2) \rangle \approx 1.51$ W.u. B) $\Delta T=0$ ; $T_Z \neq 0$ . $\langle B(E2) \rangle \approx 1.29$ W.u. C) $\Delta T=0$ ; $T_Z = 0$ . $\langle B(E2) \rangle \approx 1.3$ W.u. D) $\Delta T = \pm 1$ ; $\Delta T_Z = 0$ . $\langle B(E2) \rangle \approx 1.2$ W.u.
<u>E3-transitions</u>
A) $\Delta T=0$ ; $T_Z \neq 0$ . $\langle B(E3) \rangle \approx 4$ W.u. B) $\Delta T=0$ ; $T_Z = 0$ . $\langle B(E3) \rangle \approx 8$ W.u. C) $\Delta T = 0$ ; $\Delta T_Z = 0$ . $\langle B(E3) \rangle \approx 5$ W.u.
<u>M1-transitions</u>
A) T-favorable, $\Delta T = \pm 1$ . $\langle B(M1) \rangle \approx 0.35$ W.u. B) T-usual, $\Delta T=0$ . $\langle B(M1) \rangle \approx 0.1$ W.u. C) T-hindered (IS), $\Delta T=0$ ; $T_Z = 0$ . $\langle B(M1) \rangle \approx 0.008$ W.u. T-favorable (IV), $\Delta T = 1$ ; $T_Z = 0$ . $\langle B(M1) \rangle \approx 0.2$ W.u. Hindrance factor $\approx 20$ for IS transitions D) All, $\Delta T = 0, \pm 1$ ; $\Delta T_Z = 0$ . $\langle B(M1) \rangle \approx 0.1$ W.u.
<u>M2-transitions</u>
A) T-favorable, $\Delta T = \pm 1$ . $\langle B(M2) \rangle \approx 1.23$ W.u. B) T-usual, $\Delta T=0$ ; $T_Z \neq 0$ . $\langle B(M2) \rangle \approx 0.42$ W.u. C) T-hindered (IS), $\Delta T=0$ ; $T_Z = 0$ . $\langle B(M2) \rangle \approx 0.056$ W.u. T-favorable (IV), $\Delta T = \pm 1$ ; $\Delta T_Z = 0$ . $\langle B(M2) \rangle \approx 1.9$ W.u. Hindrance factor $\approx 30$ for IS transitions



It is necessary to have proper consideration of the soft mode [1-3] with different multipolarity for halo states and halo-halo  $\gamma$ -transitions. Up to now the halo structure has been detected for fairly considerable number of nuclei, and the list of halo nuclei continues to expand. The following halo nuclei have been selected as an initial (parent (2)) nucleus in isobar chains:  $n$ - $n$  halo –  ${}^6\text{He}$ ,  ${}^{11}\text{Li}$ ,  ${}^{12,14}\text{Be}$ ,  ${}^{17}\text{B}$ ;  $p$ - $n$  halo -  ${}^6\text{Li}$ ;  $n$  halo –  ${}^{11}\text{Be}$ ,  ${}^{14}\text{B}$ ,  ${}^{17,19}\text{C}$ ;  $p$ - $p$  halo –  ${}^{10}\text{C}$ ,  ${}^{17}\text{Ne}$ ;  $p$  halo –  ${}^8\text{B}$ ,  ${}^{12}\text{N}$ ,  ${}^{17}\text{F}$ . Using an available body of evidence [20–28] on  $\gamma$ -decay for  $6 \leq A \leq 17$  nuclei, we selected halo (intermediate halo) – halo (intermediate halo)  $\gamma$ -transitions.  $B(M, \lambda)$  and  $B(E, \lambda)$  (Table 6) for such types of  $\gamma$ -transitions are fairly large near the upper limit (Table 2) within selected nuclear region. This implies high overlapping (especially for M1 transitions) of wave functions of the initial and final states of nuclei undergoing  $\gamma$ -transition.

Table 6. Halo (intermediate halo)  $\rightarrow$  halo (intermediate halo)  $\gamma$ -transitions.

N	Nuclei/ $\gamma$ -transition. $[T_{1/2}(\text{s}) \times \Gamma(\text{eV})] = 4.8 \cdot 10^{-16}$ .
1.	${}^6\text{Li}$ , IAS, $E_{\text{lev}} = 3.56$ MeV(resonance), $I^\pi = 0^+$ , $T=1 \rightarrow {}^6\text{Li}$ , g.s., $I^\pi = 1^+$ , $T=0$ , $S_n = 5665$ keV, $S_p = 4593$ keV, $S_d = 1474$ keV. $B(M1) = 8.6$ W.u., $T_{1/2} = 5,9 \cdot 10^{-17}$ s.
2.	${}^9\text{Be}$ , $S_n = 1665.4$ keV, $S_p = 16888.2$ keV; $E_{\text{lev}} = 1.68$ MeV(resonance), $I^\pi = 1/2^+$ , $\rightarrow$ g.s., $I^\pi = 3/2^-$ , $B(E1) = 0.22$ W.u., $\Gamma_\gamma = 0.30$ eV.
3.	${}^8\text{B}$ , $S_n = 13020$ keV, $S_p = 137.5$ keV; $E_{\text{lev}} = 0.7695$ MeV (resonance), $I^\pi = 1^+$ , $\Gamma_\gamma = 0.0252$ eV $\rightarrow$ g.s. $I^\pi = 2^+$ , $B(M1) = 2.63$ W.u.
4.	${}^{10}\text{C}$ , $S_n = 21283.1$ keV, $S_p = 4006.0$ keV, $S_{2p} = 3820.9$ keV; $E_{\text{lev}} = 3.353.6$ MeV, $I^\pi = 2^+$ , $\rightarrow$ g.s. $I^\pi = 0^+$ , $B(E2) = 9.6$ W.u. $T_{1/2} = 155$ fs ( $4,25 \cdot 10^{-3}$ eV).
5.	${}^{10}\text{Be}$ , $S_n = 6812$ keV, $S_p = 19636$ keV; $E_{\text{lev}} = 7371$ keV (resonance), $I^\pi = 3^- \rightarrow E_{\text{lev}} = 5958$ keV, $I^\pi = 2^+$ , $B(E1) = 0.12$ W.u., $\Gamma_\gamma = 0.11$ eV.
6.	${}^{11}\text{Be}$ , $S_n = 501.62$ keV, $S_p = 20165$ keV; $E_{\text{lev}} = 320$ keV, $I^\pi = 1/2^- \rightarrow$ g.s., $I^\pi = 1/2^+$ , $B(E1) = 0,36$ W.u., $T_{1/2} = 115$ fs.
7.	${}^{10}\text{B}$ , $S_n = 8436.3$ keV, $S_p = 6585.9$ keV; $E_{\text{lev}} = 6875$ keV(resonance), $I^\pi = 1^-$ , $T=0+1$ (mixture), $\rightarrow E_{\text{lev}} = 5919$ keV, $I^\pi = 2^+$ , $T=0$ , $B(E1) = 0,19$ W.u. (due to isospin mixture), $\Gamma_\gamma = 0.054$ eV.
8.	${}^{17}\text{F}$ , $S_n = 16800$ keV, $S_p = 600.27$ keV; $E_{\text{lev}} = 495$ keV, $I^\pi = 1/2^+$ , $\rightarrow$ g.s. $I^\pi = 5/2^+$ , $B(E2) = 25$ W.u. $T_{1/2} = 286$ ps

Table 7. Halo (intermediate halo)  $\rightarrow$  no halo  $\gamma$ -transitions.

N	Nuclei/ $\gamma$ -transition
1.	${}^{10}\text{B}$ , $S_n = 8436.3$ keV, $S_p = 6585.9$ keV; $E_{\text{lev}} = 5919$ keV, $I^\pi = 2^+$ $\rightarrow$ g.s., $I^\pi = 3^+$ , $B(M1) = 0.026$ W.u. $\Gamma_\gamma = 0.112$ eV; $\rightarrow E_{\text{lev}} = 718$ keV, $I^\pi = 1^+$ , $B(M1) = 0.0085$ W.u., $\Gamma_\gamma = 0.025$ eV.
2.	${}^{10}\text{Be}$ , $S_n = 6812$ keV, $S_p = 19636$ keV; $E_{\text{lev}} = 5958,39$ keV, $I^\pi = 2^+$ , $T_{1/2} \leq 55$ fs (>90%) $\rightarrow E_{\text{lev}} = 3368$ keV, $I^\pi = 2^+$ , $B(M1) \approx 0.03$ W.u.
3.	${}^{14}\text{N}$ , $S_n = 10553.3$ keV, $S_p = 7550.6$ keV; $E_{\text{lev}} = 6.20$ MeV, $I^\pi = 1^+$ $\rightarrow$ g.s., $I^\pi = 1^+$ , $B(E2) = 0.021$ W.u., $B(M1) = 0,0018$ W.u., $T_{1/2} = 160$ fs.
4.	${}^{14}\text{N}$ , $S_n = 10553.3$ keV, $S_p = 7550.6$ keV; $E_{\text{lev}} = 9.13$ MeV(resonance), $I^\pi = 3^+$ , $T_{1/2}(\gamma) = 45$ fs. $\rightarrow$ g.s., $I^\pi = 1^+$ , $B(E2) = 0.0081$ W.u.; $\rightarrow E_{\text{lev}} = 5.83$ MeV, $I^\pi = 3^-$ , $B(E1) = 6.4 \cdot 10^{-5}$ W.u.; $\rightarrow E_{\text{lev}} = 6.45$ MeV, $I^\pi = 3^+$ , $B(M1) = 2.2 \cdot 10^{-3}$ W.u.
5.	${}^{14}\text{N}$ , $S_n = 10553.3$ keV, $S_p = 7550.6$ keV; $E_{\text{lev}} = 9.70$ MeV(resonance), $I^\pi = 1^+$ , $\Gamma_\gamma = 0.06$ eV $\rightarrow$ g.s., $I^\pi = 1^+$ , $B(M1) = 0.00094$ W.u.; $\rightarrow E_{\text{lev}} = 2.31$ MeV, $I^\pi = 0^+$ , $T = 1$ , $B(M1) = 5.1 \cdot 10^{-3}$ W.u.

As a next step, we selected excited states of nuclei whose characteristics were suitable for halo formation (low binding energy and angular momentum),  $\gamma$ -decay was hindered, multipolarity of transitions was small, and the final state of  $\gamma$ -decay had *a fortiori* a non-halo structure (large binding energy). The data on  $\gamma$ -decay of halo (intermediate halo)–non-halo type are presented in Table 7.

The comparison of data from Tables 6 and 7 shows that the reduced probabilities of halo–non-halo  $\gamma$ -transitions (Table 7) are far lower than those of halo–halo  $\gamma$ -transitions (Table 6). The hindrance factor can reach  $10^4$  for M1  $\gamma$ -transitions,  $5 \cdot 10^4$  for E1  $\gamma$ -transitions, and  $10^2$  for E2  $\gamma$ -transitions.

## CONCLUSIONS

1. Such excited states and resonances as isobar analog, double isobar analog, configuration states, and double configuration states in halo nuclei can also have a halo like structure of different types (*n-n*, *p-p*, *p-n*).

2. Isobar analog, double isobar analog, configuration states, and double configuration states can simultaneously have *n-n*, *n-p*, and *p-p* halo components in their wave functions.

3. The ground state of atomic nucleus  ${}^6\text{Li}$  ( $J = 1^+$ ,  $S_n = 5.66$  MeV,  $S_p = 4.59$  MeV,  $S_d = 1.47$  MeV) is a good candidate for halo state of tango type. A large value of the reduced probability of M1  $\gamma$ -transition from IAS to the ground state is evidence for the existence of tango halo structure in the  ${}^6\text{Li}$  ground state.

4. For  $A=6-19$  nuclei the hindrance factor of M1  $\gamma$ -transitions is up to  $10^4$  for halo  $\rightarrow$  no halo in comparison with halo  $\rightarrow$  halo  $\gamma$ -transitions, hindrance factor of E1  $\gamma$ -transitions is up to 50000 for halo  $\rightarrow$  no halo in comparison with halo  $\rightarrow$  halo  $\gamma$ -transitions, hindrance factor of E2  $\gamma$ -transitions is up to  $10^2$  for halo  $\rightarrow$  no halo in comparison with halo–halo  $\gamma$ -transitions.

5. Differences in halo structure of the excited and ground states (or between excited states) can result in the formation of isomers (halo-isomers).

## REFERENCES

1. *Tanihata I.* Neutron halo nuclei // J. Phys. G: Nucl. Part. Phys. **22**. (1996) 157.
2. *Jensen A.S. et al.* Structure and reactions of quantum halos // Rev. Mod. Phys. **76** (2004) 215.
3. *Jonson B.* Light Dripline Nuclei // Physical Reports **389** (2004) 1.
4. *Zhukov M.V. et al.* Bound state properties of Borromean halo nuclei:  ${}^6\text{He}$  and  ${}^{11}\text{Li}$  // Phys. Rep. **231** (1993) 151.
5. *Suzuki Y., Yabana K.* Isobaric analogue halo states // Phys. Lett. B **272** (1991) 173.
6. *Zhihong L. et al.* First observation of neutron-proton halo structure for the 3.563 MeV  $0^+$  state in  ${}^6\text{Li}$  via  ${}^1\text{H}({}^6\text{He}, {}^6\text{Li})n$  reaction // Phys. Lett. B **527** (2002) 50.
7. *Naumov Yu.V., Kraft O.E.* Isospin in Nuclear Physics, Nauka, Moscow, Leningrad, 1972.
8. *Izosimov I.N.* Structure of the isobar analog states (IAS), double isobar analog states (DIAS), and configuration states (CS) in halo nuclei // Proc. Int. Conf. EXON2012, Vladivostok, Russia, World Scientific, 2013, P.129. *Joint Institute for Nuclear Research, Preprint* E6-2012-121, Dubna (2012).
9. *Izosimov I.N.* Isobar analog states (IAS), double isobar analog states (DIAS), configuration states (CS), and double configuration states (DCS) in halo nuclei. Halo isomers // Proceedings of the International Conference Nuclear Structure and

- Dynamics III, Portoroz, Slovenia, 2015. AIP Conference Proceedings, 2015, V. **1681**, P. 030006. Preprint No E6-2015-41, JINR (Dubna, 2015).
10. *Izosimov I. N.* Borromean halo, Tango halo, and halo isomers in atomic nuclei//Proceedings of the International Conference Nuclear Structure and Related Topics (NSRT 2015), Dubna, Russia, 2015. EPJ Web of Conferences, 2016, V.**107**, P. 09003.
  11. *Ogloblin A.A. et al.* Observation of neutron halos in the excited states of nuclei // Int. Journ. of Mod. Physics E, **20** (2011) 823.
  12. *Chen Jin-Gen. et al.* Proton Halo or Skin in the Excited States of Light Nuclei // Chin. Phys. Lett., **20** (2003) 1021.
  13. *Naumov Yu.V., Kraft O.E.* Gamma-decay of the Analogue Resonances // Phys. Part. Nucl., **6** (1975) 892.
  14. *Tuli J.K.* Evaluated Nuclear Structure Data File: A Manual for Preparation of Data Sets // Report BNL-NCS-51655-01/02-Rev, 2001.
  15. *Endt P.M.* Strengths of Gamma-Ray Transitions in A=45–90 Nuclei // At. Data & Nucl. Data Tables, **23** (1979) 547.
  16. *Endt P.M.* Strengths of Gamma-Ray Transitions in A=6–44 Nuclei (III) // At. Data & Nucl. Data Tables, **23** (1979) 3.
  17. *Endt P.M.* Strengths of Gamma-Ray Transitions in A=91–150 Nuclei // At. Data & Nucl. Data Tables, **26** (1981) 47.
  18. *Kalpakchieva R. et al.* Momentum Distributions of  $^4\text{He}$  Nuclei from the  $^6\text{He}$  and  $^6\text{Li}$  Breakup // Physics of Atomic Nuclei, **70** (2007) 619.
  19. *Penionzhkevich Yu.E.* Special Features of Nuclear Reactions Induced by Loosely Bound  $^6\text{He}$  and  $^6,7\text{Li}$  Nuclei in the Vicinity of the Coulomb Barrier Height // Physics of Atomic Nuclei, **72** (2009) 1617.
  20. National Nuclear Data Center, Brookhaven National Laboratory.  
<http://www.nndc.bnl.gov>
  21. *Tilley D.R. et al.* Energy Levels of Light Nuclei A = 6 // Nuclear Physics A, **708** (2002) 3.
  22. *Kelley J.H. et al.* Energy Levels of Light Nuclei A = 11 // Nuclear Physics A, **880** (2012) 88.
  23. *Tilley D.R. et al.* Energy levels of light nuclei A = 5, 6, 7 // Nuclear Physics A, **708** (2002) 3.
  24. *Tilley D.R. et al.* Energy levels of light nuclei A = 8, 9, 10 // Nuclear Physics A, **745** (2004) 155.
  25. *Ajzenberg-Selove F.* Energy levels of light nuclei A =11–12 // Nuclear Physics A, **506** (1990) 1.
  26. *Ajzenberg-Selove F.* Energy levels of light nuclei A =13–15 // Nuclear Physics A, **523** (1991) 1.
  27. *Tilley D.R. et al.* Energy levels of light nuclei A = 16–17 // Nuclear Physics A, **565** (1993) 1.
  28. *Tilley D.R. et al.* Energy Levels of Light Nuclei A = 18–19 // Nuclear Physics A, **595** (1995) 1.
  29. *Soloviev V.G.* Theory of Atomic Nuclei: Quasiparticles and Phonons, Institute of Physics, Bristol and Philadelphia, 1992.